J-integral measured from experimental torque load versus torque-ends rotation angle obtained from a spiral notch torsion test*

Jy-An Wang

Materials Science and Technology Division, Oak Ridge National Laboratory, 1 Bethel Valley Road, Oak Ridge, Tennessee 37831, USA, email: wangja@ornl.gov

ABSTRACT

Spiral Notch Torsion Test (SNTT) was developed to measure the intrinsic fracture toughness of structural materials using small specimens. The SNTT system operates by applying pure torsion to cylindrical specimens with a notch line that spirals around the specimen at a 45° pitch. 3-D finite-element analysis has been used to estimate the fracture toughness obtained from SNTT test specimen with 3-D non-coplanar crack front. Here a newly developed SNTT protocol to estimate J-integral directly from the experimental torque load versus torque-ends rotation angle trend curve without the aid of 3-D finite element analyses is presented and its applicability is illustrated by applying it for the evaluation of fracture toughness of SS304/308 weldment. The estimated J_Q' for the SS304/308 weld is 144.2 kJ/m², which is consistent with that obtained from CT specimen.

Keywords—fracture toughness; spiral notched torsion test; miniature specimen; J-integral

Nomenclature: a, crack length; b, unbroken ligament; B, crack front length; D, diameter; θ_{total}, torque end rotation angle, θ_{nc}, rotation angle without cracks; θ_c, rotation angle due to the introducing the crack; γ, the unit end rotation angle; μ is the shear modulus; A, area under torque load-rotation angle curve; U, potential energy; W, strain energy density function; $J_{Q'}$, J-integral value upon catastrophic fracture; K_{IC}, Mode I fracture toughness; R, cylinder radius; Tq, applied torque; σ, the stress tensor; u, the displacement vector; Γ, a contour surrounding the crack tip; n_j, direction cosines of the outward normal on Γ; ds, an infinitesimal arc length along Γ.

1. INTRODUCTION

Adequate toughness is an essential consideration of structural systems design. The American Society for Testing and Materials (ASTM) standard test methods, *Standard Test Method for Plane-Strain Fracture Toughness of Metallic Materials* (E399) [1], are widely used to determine fracture toughness of metallic materials, using compact tension and compact disk tension specimens having thickness and volume sufficiently large to ensure the plane-strain condition at the crack front. However, meeting these requirements is often difficult when the material/sample may be geometrically unsuitable and/or have insufficient volume for fabricating the standard specimen. Therefore, use of small specimens for fracture toughness measurement is essential, and SNTT approach was developed to meet these needs.

Despite the international efforts on the development of small specimen testing techniques, no methods currently exist for direct measurement of fracture toughness for small specimens without a concern for size effect. Unlike the conventional test methods, the SNTT method is capable of testing small rod specimens that bear no resemblance to conventional compact tension specimens nor using conventional mode of loading.

2. SPIRAL NOTCH TORSION TEST SYSTEM

SNTT System (Fig. 1) was developed for determining fracture toughness values for a wide spectrum of materials ranging from ductile to brittle materials. Test results obtained for steel, aluminum, stainless steel, graphite and mullite ceramic were compared and validated with those reported in the open literature [2-10]. The SNTT test system operates by applying pure torsion to cylindrical specimens having a notch line that spirals around the specimen at a 45° pitch angle. The pure torsion creates a uniform equibiaxial tension/compression stress field on each of concentric cylinders and the grooved line effectively becomes a Mode I crack mouth opening. It is not difficult to visualize that the rod specimen is a different manifestation of a compact-tension specimen having a thickness equivalent to the total length of the spiral notch. Compact-tension specimen testing lacks a method to uniformly distribute applied load throughout the entire specimen thickness because the stresses at and near the two free surfaces are anomalous, resulting in shear lip formation often discernible in fractured specimens. In contrast, the torque load acting on every cross-section along the rod specimen is the same and directly measurable. A plane-strain condition is achieved on every plane normal to the spiral groove. Because of the plane strain, axisymmetric constraint and the uniformity in the stress and strain fields, the crack front must propagate perpendicularly toward the specimen axis along the conoids (Fig. 2). Post-mortem examination verified the crack propagation behavior (Fig. 3). Thus, the crack growth characteristics are controllable, and *fracture toughness* can be determined reliably. K_{IC} estimated from the SNTT method are virtually independent of specimen size; this make miniaturization an important goal of SNTT method.

2.1 The development of SNTT compliance function for ductile materials

Applying SNTT method to ductile materials, it is essential to develop SNTT fatigue crack growth procedures, in addition to a single notch-front geometry. An integrated experimental and analytical approach [11] was used to study the SNTT crack growth behavior. The non-dimensional index associated with the rotational compliance of the SNTT sample were used to estimate the SNTT crack growth. The evolutions of the SNTT specimen rotational compliance during the crack growth can be unified together irrespective of specimen sizes and material types [11], as shown in Fig. 4 for steel and aluminum materials with sample diameters of 9.525-mm and 25.4-mm. The evolutions of rotational compliance in SNTT crack growth were formulated as function of the ratios of crack lengths vs. the cylindrical diameter, as shown in Fig. 4; where γ is the unit end rotation angle; T is the applied torque; μ is the shear modulus; and R is the cylinder radius. This developed compliance function was used to determine the fatigue pre-crack growth length. Experimental verification on the developed protocol were carried out on SS304/308 weld SNTT samples. The SNTT fatigue crack penetration depths were measured and compared with predictions obtained from the SNTT rotational compliance governing equation.

The developed compliance functions are essential to SNTT approach to effectively develop a controllable fatigue crack growth testing protocol. For specimen ends' rotational angle measurement obtained from the Rotary Variable Differential Transformer (RVDT) of the biaxial tester, the developed compliance function needs to be benchmarked with the deformation of the pre-fatigue SNTT baseline notch specimen to determine the SNTT sample effective gage length, used to normalize the rotation angle. However, if a biaxial extensometer was used in the sample gage section for rotation angle estimate, then the benchmark procedure based on the pre-notch baseline SNTT sample would not be needed.

3. SNTT WELD SAMPLE PREPARATION AND BIAXIAL TESTER SET-UP

3.1 The received Sandia canister weldment

The received canister weldment samples are from the top portion of the Cut B section [12], which are made of the 304/304L SS plates and the 308L SS filler material. All the welds of the mockup canister were formed using the submerged-arc welding (SAW) process with multi-pass welds [12]. The tensile properties of the 304, 304L, 308L SS plates, and SS304/308 weld materials are stated in Table 1 [13,14].

Table 1 Stainless steel mechanical properties

Type	E [GPa]	0.2% Yield stress [MPa]	UTS [MPa]
304	195	241	586
304L	195	207	552
308L	195	207	551
304/308 SAW	195	380	565

3.2 SNTT weld specimen designs and configurations

SNTT samples were fabricated from several as-received Sandia canister SS 304/308 weld plates. The thickness of the weldment is 15.87-mm, and the diameter of the SNTT cylinder was designed to be 9.53-mm accordingly (Fig. 5a). The SNTT specimen axis was parallel or perpendicular to the canister cylinder axis, pending on the received weldment is axial or circumferential weld. There are several types of spiral grooves designs with different notch depths, as illustrated in Fig. 5b. The weld specimen has its centerline aligned with the center of fusion zone. For the deep notch weld samples two loops spiral groove was also designed. Threads were introduced onto both ends of the SNTT samples. Normally, deep-notch SNTT specimen can provide a higher constraint environment for the crack front compared to that of a shallow-notch starter. Thus, deep-notch specimen can significantly reduce the load capacity and cyclic number required to reach the targeted fatigue crack length for a ductile metal.

3.3 SNTT equipment setup

Preliminary calculations estimate that the threshold of crack initiation in these samples with shallow notch of 0.9525-mm is around 31.64 Nm. The maximum capacity of the torque load provided by the Test Resource 830 axial-torsion machine is 183 N-m. The cyclic fatigue frequency can reach 10 HZ range under the targeted torque load range. These specifications ensure that cycle fatigue testing of SNTT SS304/308 weld steel specimens can be conducted, in addition to the final SNTT fatigued sample fracture testing. The detailed SNTT tester set-up is shown in Fig. 6.

The preliminary estimate for the threshold of crack initiation was based on SS weld yield criterion on a SNTT sample surface, where the maximum shear stress profile for the notch cylinder specimen was estimated according to the simplified shear stress equations. Maximum allowable shear stress upon yield was estimated from the tensile yield stress of SS 304/308 weld. The torque load that can produce 60-80% of the maximum allowable shear stress on SNTT sample surface was used as the initial driving force to induce fatigue crack growth.

4. CANIASTER SS304/308 WELD FRACTURE TOUGHNESS EVALUATION

4.1 SNTT testing on ss304/308 weld steel material

4.1.1 Cycle fatigue process

The cycle fatigue process on SS304/308 weld SNTT samples were performed through the angle control mode by a function generator built in the TestResource control system. The selected initial fatigue cyclic loading is the torque that can reach about 60-80% of the maximum allowable shear stress level on the specimen surface. This is to ensure a linear elastic deformation existed during the fatigue cycling. In order to find the optimized fatigue threshold of the SS304/308 SNTT samples, the initial maximum torque was adjusted to approximately 30.5 N-m with 5 HZ cyclic fatigue process. This cyclic load was gradually increased to facilitate the crack growth in a reasonably time frame to reach the targeted total crack growth length ("a", notch depth plus the fatigue crack growth length); where the targeted a/D is normally in the ranges of 0.35 to 0.45. The crack growth during the fatigue cycles was monitored by the specimen's compliance or stiffness changes and then using the developed compliance function to estimate the crack penetration depth.

4.1.2 Monotonic loading fracture test

Fatigued SNTT sample was then loaded monotonically using the biaxial tester with series of loading/unloading sequences until failure; where the loading rate of 0.248 N-m/second and unloading rate of 2.0 N-m/second were used. The monotonic loading rates for ramping loading and unloading sequences were carried out under load control in each loading/unloading sequence to reach the target loading and the specified unloading range (normally about 10-15% reduction in maximum load in each loading/unloading sequence). During the monotonic loading/unloading period, the axial force is maintained at nil zero condition to ensure a pure torsion loading condition. Upon final sudden fracture failure, a significant axial shock reaction force was observed, which was used to determine the final fracture torque load. The typical experimental test results for SNTT 304/308 weld samples are shown in Fig. 7. Fig 7 shows a 2-loop deep-notch Weld-9 test results, the specimen failed at 38.2 N-m torque.

4.1.3 Failed sample characterization

The failed SNTT samples were characterized using an optical camera, which captured optical images of the specimen and the fractured surfaces, as shown in Fig. 8 for the tested 2-loop Weld-10 SNTT sample. Fig. 8b shows that the 2-loop Weld-10 SNTT sample fractured into two halves during the monotonic loading. The failed surfaces from matching surfaces indicate a significant crack tip blunting occurred before the

specimen final fracture. The fatigue pre-crack length is at 1.028-mm and the notch depth is at 2.857-mm; the total crack length ratio, a/D, is equal to 0.40. The fractured surface profile shows smooth pre-crack growth surface and the final fast fracture topology characteristic under monotonic loading.

4.1.4 SNTT 304/308 weld samples fracture test results

The details of the SNTT 304/308 weld samples test results are illustrated in Table 2; where most weld specimens failures were initiated near heat-affected zone (HAZ) region, and all the two loops weld samples were failed at or near HAZ regions, as shown in Fig. 9a. Table 2 shows that the fracture torques from different tests appear to be self-consistent at the targeted a/D ratio, which indicates the good repeatability of the SNTT methodology in applying to the highly ductile SS304/308 weld materials. The large axial bending distortion observed from the fractured 2-loop deep-notch specimens is due to significant axial shock reaction force upon SNTT specimen catastrophically fractured and broken into two pieces. Fig 9b shows a SNTT 2 loop Weld-8 specimen fracture test results, sample failed at 39.5 N-m, and upon failure significant axial shock reaction load was observed, at magnitude of ~380 N. This shock reaction load was also used to pinpoint/determine the maximum fracture load.

Table 2 SNTT 304/308 weld specimens and 304 base specimen fracture test results

Sample ID	Spiral groove loop	Notch depth, a_0 mm	Gage length, GL mm	Total crack length, a mm	a/D	Uncracked ligament, b mm	Crack front length, B* mm	Fracture Torque N-m
Weld-1	1	1.91	23.92	3.34	0.350	6.19	25.55	56.0
Weld-5	1	2.54	13.46	4.23	0.440	5.30	13.87	38.5
Weld-8	2	2.86	23.92	3.96	0.416	5.56	25.95	39.5
Weld-9	2	2.86	23.92	4.00	0.420	5.52	25.77	38.2
Weld-10	2	2.86	23.92	3.89	0.408	5.64	26.33	41.0
Base	2	2.86	23.92	3.77	0.396	5.75	26.97	45.0

*Single loop B: $\sqrt{[(2\pi(R-a))^2+GL^2]}$,
*Double loop B: $\sqrt{[4(2\pi(R-a))^2+GL^2]}$, R is radius.

4.2 Fracture toughness evaluation on the tested SNTT SS304/308 weld samples

4.2.1 SNTT finite element modeling methodology for ductile materials

The methodology used for developing finite element model (FEM) and the typical FEM analyses results are illustrated in Fig. 10. The FEM designed for the ductile material SNTT fatigue pre-crack sample characterization was used for demonstration. Due to high ductility of the SS304/308 weld material, the

singular wedge element with quarter-node elements around the crack tip was relaxed back to normal wedge element with middle-node elements. The typical FEM analyses results are also shown in Fig. 10, where the tri-axial tensile stress profiles (observed up to 8-th elements from the crack front) and the butterfly plastic process zone indicate a high geometry constraint condition exists in the proposed SNTT fracture toughness testing protocol.

The Abaqus J-integral contour routine was used in the J-integral value evaluation. The same routine was used for toughness evaluation of A533B and A302B alloy steels in the past [2,3] and reaches good agreements compared to conventional CT test results. The procedure of FEM approach used in $J_{Q'}$ evaluation is stated as following: The FEM model was developed using FEM mesh generator, to match the SNTT sample geometry and the associated boundary conditions, such as the crack front profile, the total crack length, and SNTT sample geometry constraints. Final fracture torque obtained from SNTT experiment was used as load input in FEM model. In general, the unit rotation angle and the overall deformation obtained from the FEM results are quite consistent with that of SNTT experimental test results.

4.2.2 FEM analyses and energy release rate evaluation for SNTT Weld-10 specimen test results

Total 89,603 nodes and 21,280 3-D solid reduced-integration elements were used to model SNTT Weld-10 specimen with a crack length of 3.886-mm. The fractur torque is at 41.0 N-m. The deformed FEM model upon failure and the associated von Mises stress contours are shown in Fig. 11. The estimated $J_{Q'}$ for SNTT 304/308 Weld-10 specimen upon final fracture is 148.8 KJ/m^2.

4.3 Comparison between SNTT and Compact Tension (CT) Tests Results for Fracture Toughness Evaluation

The comparison of SNTT 304/308 weld fracture toughness (represented with J-integral value at final fracture load, $J_{Q'}$) and the mean J_{IC} obtained from conventional CT test [15] are illustrated in Table 3; where SNTT weld test samples uncertainty bond evaluation was performed on the targeted a/D in the range of 0.40 to 0.42. Table 3 shows that the SNTT estimated mean $J_{Q'}$ is very close to the mean J_{IC} obtained from the CT method for the weld specimens.

Table 3 Summary of fracture toughness obtained from SNTT test and CT test results

Method	Material	Condition	Temperature C°	Mean J_{IC} KJ/m²	Mean $J_{Q'}$ KJ/m²	Standard deviation KJ/m²

CT	304/308	SAW	21	147.0		67.0
SNTT	304/308	SAW	21		140.6	8.8

5. SEMI-EMPIRICAL APPROACH TO EVALUATE J-INTEGRAL FOR SNTT SPECIMENS

The J-integral represents a way to calculate the strain energy release rate, or work (energy) per unit fracture surface area, in a material [16,17]. In 1968 J. R. Rice published papers in which he discussed the potential of a path-independent integral, J, for characterizing fracture in non-linear-elastic materials.

The *J*-integral has been shown to be equivalent to the rate of release of the potential energy U with respect to the crack extension [16]: for a body of thickness B,

$$J = -\frac{1}{B}\frac{\partial U}{\partial a} \tag{1}$$

Where, *a* represents crack length, and represents the system potential energy. An alternate and equivalent definition of J can be written as follow [18],

$$J = \frac{1}{B}\int_0^{\Delta}\left(-\frac{\partial P}{\partial a}\right)_{\Delta} d\Delta, \qquad \text{or,} \qquad J = \frac{1}{B}\int_0^{P}\left(\frac{\partial \Delta}{\partial a}\right)_{P} dP, \tag{2}$$

These representations relate J to the rate of change with respect to crack size, a, of the area under the load versus load-point-displacement, P versus Δ, curves. Here P is the force and the curves are generated for different crack sizes, a, where specimens subjected to monotonic loading. This definition was used by Begley and Landes in the experimental evaluation of the J versus Δ relation [19]. Rice first recognized that for configuration with a single characteristic dimension dominating the deformation behavior such as uncracked ligament, $b = W - a$ [18]. For a deeply cracked SNTT specimen, the relative additional angle of the grip end rotation due to the presence of the crack, θ_c, can be estimated from a dimensional analysis. Consider a SNTT rod specimen with diameter, *D*, subjected to a pure torsion force, T_q, which is transmitted through a narrow neck of width, $b = D - a$, between spiral crack front and the cylinder free surface edge. The torque end rotation angle, θ_{total}, can be regarded as the sum of the rotation angle without cracks, θ_{nc}, plus the rotation angle due to the introducing the crack, θ_c, i.e., $\theta_{total} = \theta_{nc} + \theta_c$. For an applied torque Tq of SNTT configuration with spiral crack front length, B, θ_c can be expressed as,

$$\theta_c = f\left(\frac{T_q}{Bb}\right) \tag{3}$$

and, J-integral can be represented as

$$J = \frac{1}{Bb}\int_0^{\theta_c} T_q d\theta_c \quad \text{or,} \quad J = \frac{1}{Bb}\int_0^{\theta_{total}} T_q d\theta_{total} \tag{4}$$

where, $\int_0^{\theta_c} T_q d\theta_c$ is the area under the T_q - θ_c curve.

The detailed derivation of semi-empirical J-integral representation for SNTT specimen under pure torsion loading is described in Appendix section.

6. J-INTEGRAL EVALUATION FOR SS 304/308 WELDMENT MATERIAL

The J-integral evaluation results based on $J = \frac{1}{Bb}\int_0^{\theta_c} T_q d\theta_c$ for the SS304/308 weld SNTT samples and SS304 base SNTT sample are illustrated in Tables 4. Where load-displacement area under torque load - rotation angle trend curve is shown in Fig. 12. Table 4 shows the mean J-integral upon fracture for SS304/308 weld and SS304 base are 144.2 KJ/m² and 459.0 KJ/m², respectively.

Table 4 SNTT 304/308 weld & SS304 base specimens fracture toughness test results

Sample ID	Spiral groove loop	Notch depth, a_0 mm	Gage length, GL mm	Total crack length, a mm	a/D	Uncracked ligament, b mm	Crack front length, B mm	Fracture Load, Tq N-m	Tq - θ area, A KJ	J-integral, A/bB KJ/m²
Weld-1	1	1.91	23.92	3.34	0.350	6.19	25.55	56.0	24.50	154.9
Weld-5	1	2.54	13.46	4.23	0.440	5.30	13.87	38.5	9.56	130.1
Weld-8	2	2.86	23.92	3.96	0.416	5.56	25.95	39.5	20.52	142.3
Weld-9	2	2.86	23.92	4.00	0.420	5.52	25.77	38.2	22.92	154.0
Weld-10	2	2.86	23.92	3.89	0.408	5.64	26.33	41.0	20.77	139.9
									Mean	144.2
									Two Sigma	±10.4
SS304 Baseline	2	2.86	23.92	3.77	0.396	5.75	26.97	45.0	71.25	459.0

6.1 J-integral Evaluation Comparison between SNTT Semi-empirical Approach and Compact Tension (CT) Tests Results

The comparison of SNTT 304/308 weld fracture toughness (represented with J-integral value at final fracture load, $J_{Q'}$) and the mean J_{IC} obtained from conventional CT test [15] are illustrated in Table 5. Table 5 shows that the SNTT estimated semi-empirical $J_{Q'}$ is very close to the mean J_{IC} obtained from the CT method for the weld specimens. Base metal CT test fracture toughness appears to be higher than that

estimated from SNTT approach; this could be due to the canister wall cold work forming process of the received canister weldment. The high uncertainty for both base and weld metals from CT tests were also observed. Due to limit SNTT base metal test conducted, no associated uncertainty study was carried out. Small uncertainty bond of SNTT approach for weld samples compared to that of CT test results could be primary due to SNTT inherited high geometry constraint and the self-consistent fracture torques observed from the SNTT fracture test results as shown in Tables 2.

Table 5 Summary of fracture toughness obtained from SNTT test and CT test results

Method	Material	Condition	Temperature	Mean J_{IC}	Mean $J_{Q'}$	Standard deviation
			C°	KJ/m²	KJ/m²	KJ/m²
CT	304 base	Base metal	21	672.0		215.0
SNTT	304 base	Base metal	21		459.0	
CT	304/308 weld	SAW	21	147.0		67.0
SNTT	304/308 weld	SAW	21		144.2	10.4

7. CONCLUSIONS

A new J-integral evaluation protocol was developed based on the measured fracture torque and torque ends rotation angle trend curve, obtained from the SNTT method. The estimated semi-emprical SNTT fracture toughness J_Q' for the SS304/308 weldment is consistent with that using conventional CT specimens. The SNTT test results indicate that SNTT method is a reliable test method with good repeatability and applicable to SS304/308 weld material. The estimated J_Q' upon fracture for the baseline SS304 steel is at 459 kJ/m². The estimated J_Q' upon fracture for the SS304/308 weld from weld specimens is 144.2 kJ/m².

The unique features of the SNTT method are:

• It conforms to the classical theory of fracture mechanics.

• It is not limited by sample size or volume.

• It controls crack propagation and thus produces consistent results.

ACKNOWLEDGMENTS

This research was funded by Spent Nuclear Fuel Canister Program of the U.S. Department of Energy and the Laboratory Directed Research and Development Program of Oak Ridge National Laboratory, managed by UT-Battelle, LLC for the US Department of Energy; and was carried out at Oak Ridge National Laboratory under contract DE-AC05-00OR22725 with UT-Battelle, LLC. The authors would like to thank Program Managers Bruce Bevard and John Scaglione for providing support to this project.

APPENDIX: J-integral for A Deep Spiral Notch Crack SNTT Specimen under Pure Torsion

For an applied torque *Tq* of SNTT configuration with the spiral crack front length, B, the θ_c can be expressed as,

$$\theta_c = f\left(\frac{T_q}{Bb}\right)$$

The torque end rotation angle, θ_{total}, can be regarded as the sum of the rotation angle without cracks, θ_{nc}, plus the rotation angle due to the introducing the crack, θ_c, i.e., $\theta_{total} = \theta_{nc} + \theta_c$. And because θ_{nc} does not dependent on crack length, *a*, then

$$\frac{\partial \theta_{total}}{\partial a} = \frac{\partial \theta_c}{\partial a}$$

Thus, J can be written as:

$$J = \frac{1}{B}\int_0^{T_q}\left(\frac{\partial \theta_c}{\partial a}\right)_{T_q} dT_q,$$

$$\left(\frac{\partial \theta_c}{\partial a}\right)_{T_q} = \left(\frac{\partial \theta_{total}}{\partial a}\right)_{T_q} = -\left(\frac{\partial \theta_{total}}{\partial b}\right)_{T_q} = -\left(\frac{\partial \theta_c}{\partial b}\right)_{T_q}$$

Replace θ_c with $f(Tq/Bb)$, and *J* can be written as:

$$J = -\frac{1}{B}\int_0^{T_q}\left(-\frac{T_q}{Bb^2}\right) f'\left(\frac{T_q}{Bb}\right) dT_q$$

where

$$f' = df/d\left(\frac{T_q}{Bb}\right)$$

$$d\theta_c = f'\left(\frac{T_q}{Bb}\right) \cdot \frac{dT_q}{Bb}$$

Hence,

$$J = \frac{1}{B}\int_0^{\theta_c} \frac{T_q}{b} d\theta_c = \frac{1}{Bb}\int_0^{\theta_c} T_q d\theta_c$$

where, $\int_0^{\theta_c} T_q d\theta_c$ is the area under the T_q - θ_c curve.

The alternative in implementing equation above is stated as following:

The full angle θ_{total} is usually measured. However, for a deeply cracked specimen, θ_{nc} is small and we can usually assume that $\theta_{total} \cong \theta_c$. Thus, J integral for SNTT approach can also be written as:

$$J = \frac{1}{Bb}\int_0^{\theta_{total}} T_q d\theta_{total}$$

REFERENCE

1. ASTM, 2004, Test Method for Plane-Strain Fracture Toughness of Metallic Materials, ASTM E 399-90, ASTM International, Philadelphia, PA.
2. J.A. Wang, K. Liu, D. McCabe, S. David, Using torsional bar testing to determine fracture toughness, Fatigue Fract Engng Mater Struct 23 (2000) 917–927.
3. J.A. Wang, K.C. Liu, A new approach to evaluate fracture toughness of structural materials. Journal of Pressure Vessel Technology, 126 (2004) 534-540.
4. J.A. Wang, I.G. Wright, M.J. Lance, K..C Liu, A new approach for evaluating thin film interface fracture toughness, Journal of Materials Science and Engineering A, 426 (2006) 332-345.
5. J.A. Wang, K. Liu, An innovative technique for evaluating fracture toughness of graphite materials. Journal of Nuclear Materials, 381 (2008) 77-184.
6. J.A. Wang, K. Liu, D. Naus, A new test method for determining the fracture toughness of concrete materials. Journal of Cement and Concrete Research, 40 (2010) 497-499.
7. T. Tan, F. Ren, J.A. Wang, E. Lara-Curzio, P. Agastra, J. Mandell, et al. Investigating fracture behavior of polymer and polymeric composite materials using spiral notch torsion test. Journal of Engineering Fracture Mechanics, 10 (2013) 109-128.
8. F. Ren, J.A. Wang, W. Bertelsen, Fractographic study of epoxy materials fractured under mode I loading and mixed mode I/III loading. Materials Science and Engineering A, 532 (2012) 449-455.
9. J.A. Wang, Fracture toughness evaluation for thin-shell stainless steel weldment, Journal of Theoretical and Applied Fracture Mechanics, 106 (2020), 102467. https://doi.org/10.1016/j.tafmec.2019.102467

10. J.A. Wang, F. Ren, T. Tan, K. Liu, The development of in situ fracture toughness evaluation techniques in hydrogen environment, International Journal of Hydrogen Energy, 40 (2015) 2013-2024.

11. J.A. Wang, T. Tan, A method for evaluating the fatigue crack growth in spiral notch torsion fracture toughness test. Archived of Applied Mechanics Journal, 89 (2019) 813–822.

12. D.G. Enos and C.R. Bryan, Final Report: Characterization of canister mockup weld residual stress, Sandia National Laboratory, November 22, 2016. FCRD-UFD-2016-000064.

13. Stainless Steels Properties – How to weld them and where to use them. The Lincoln Electric Company. http://www.lincolnelectric.com/assets/global/Products/Consumable_StainlessNickelandHighAlloy-Excalibur- Excalibur316316L-17/c64000.pdf

14. http://www.lincolnelectric.com/assets/global/Products/Consumable_StainlessNickelandHighAlloy-Lincolnweld-Lincolnweld308308L/c61024.pdf.

15. Mills WJ, Fracture toughness of type 304 and 316 stainless steels and their welds. International Materials Reviews, 42:2 (1997) 45-82, DOI: 10.1179/imr.1997.42.2.45.

16. J. R. Rice, "A path-independent integral and the approximate Analysis of strain concentration by notches and cracks," Journal of Applied Mechanics, Trans. ASME, 35 (1968) 379-386.

17. G.P. Cherapnov, "Crack propagation in continuous media," Applied Mathematics and Mechanics, (trans. P.M.M.), 31 (1967) 476-488.

18. J.R. Rice, P.C. Paris, J.G. Merkle, Some further results of J-integral analysis and estimates. Progress in flaw growth and fracture toughness testing, ASTM STP 536, 231-245, American Society for Testing and Materials, 1973.

19. J.A. Begley and J.D. Landes, The J-Integral as a fracture criterion. *Fracture Toughness*, ASTM STP 514, 1-23, American Society for Testing and Materials, 1972.

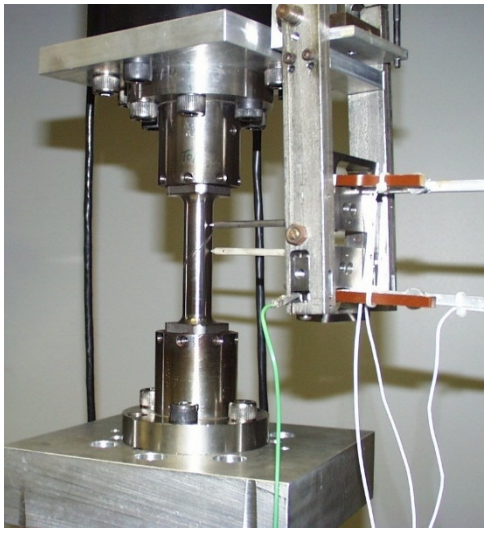

Fig. 1 SNTT test sample set-up, including the biaxial extensometer.

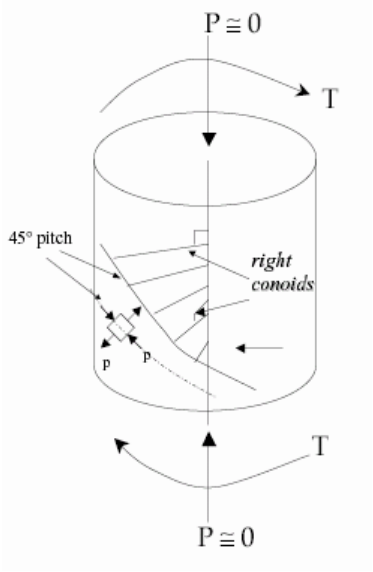

Fig. 2. Pure torsion loading schematic indicates that the principal tensile stress profile is perpendicular to the 3-D spiral contour of 45° pitch angle.

Fig. 3. Fractured contour of 7475-T7351 aluminum SNTT specimen indicates that the crack propagation orientation is perpendicular and toward the cylinder central axis.

Scaled SNTT Crack Growth Compliance Equation

$$\frac{\gamma}{T}\mu R^4 \left[1-\frac{a}{D}\right]^4 = 3.3445\left[\frac{a}{D}\right]^4 - 5.2514\left[\frac{a}{D}\right]^3 + 4.0568\left[\frac{a}{D}\right]^2 - 2.2298\left[\frac{a}{D}\right] + 0.6226$$

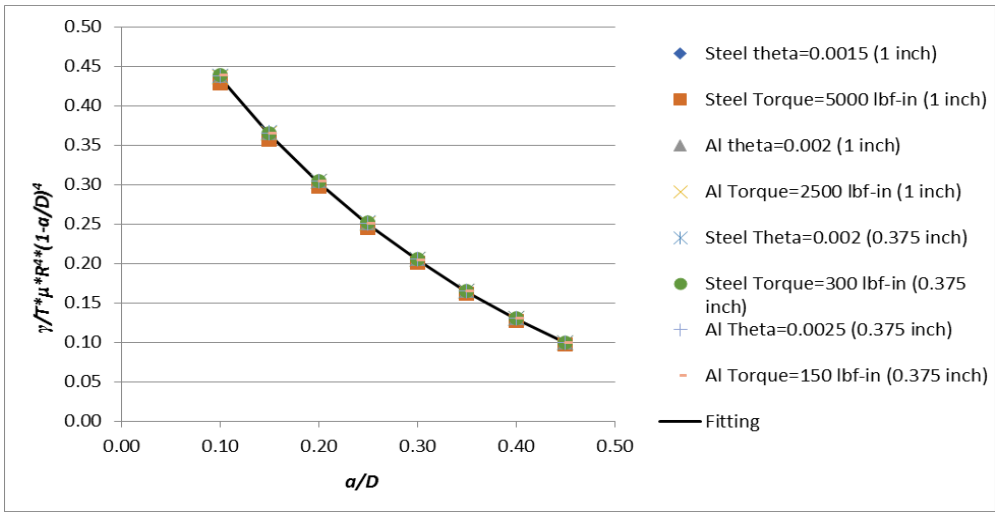

Fig. 4. The SNTT rotational compliance evolution at different crack growth length.

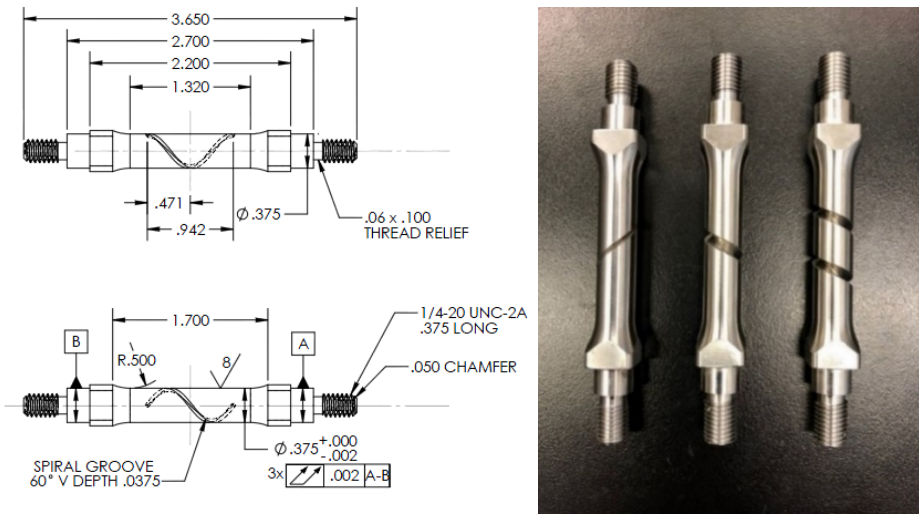

(a) **(b)**

Fig. 5. (a) Geometry details of the SS304/308 weld steel SNTT specimen; (b) SNTT specimens with different spiral groove designs, (left) single loop spiral groove with 0.953-mm (0.0375”) notch depth, (middle) single loop with 2,54-mm (0.100”) notch depth, (right) two loops with 2.86-mm (0.1125”) notch depth.

Fig. 6. (Left) SNTT biaxial tester set-up and installation of SS 304/308 weldment sample, (Right) the final fracture of tested SNTT weld sample.

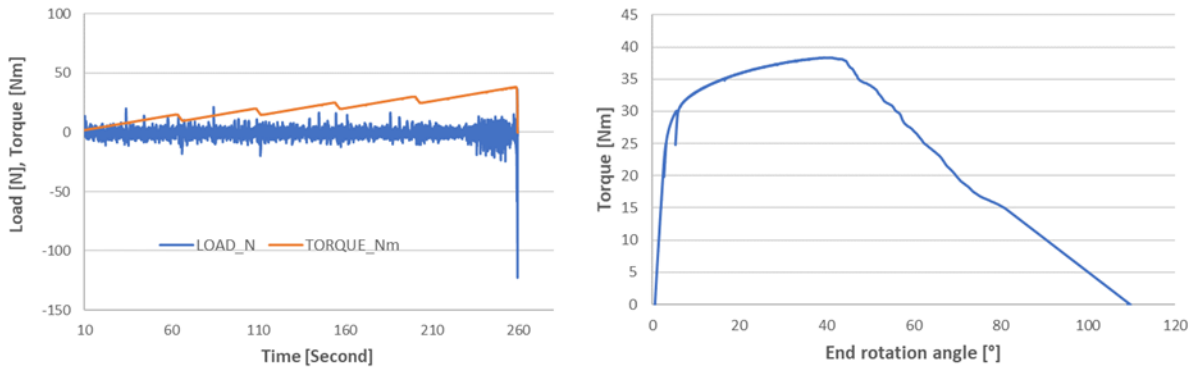

Fig. 7. Weld-9 2-loop sample test results, (left) upon sudden failure a shock reaction force was observed, (right) the slopes of different loading and unloading sequences does not change, indicate no crack growth during the monotonic loading, the specimen failed at 38.2 N-m torque.

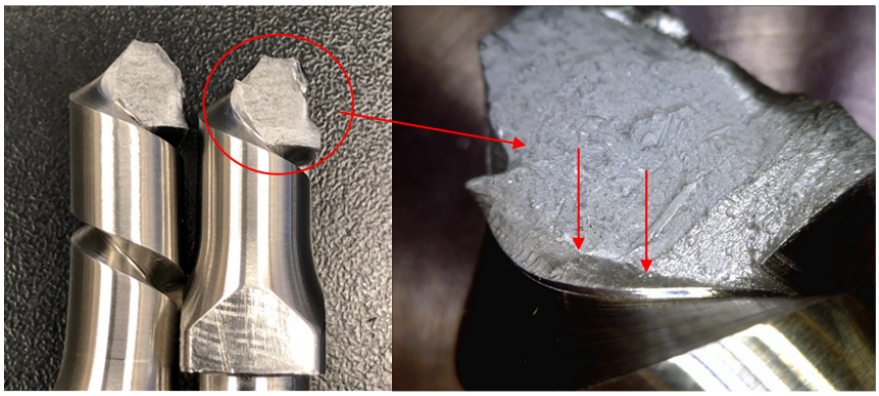

Fig. 8. SNTT 2-loop Weld-10 fracture specimen and the associated fracture surface profile, the red arrows point to the fatigue pre-crack front.

(a)

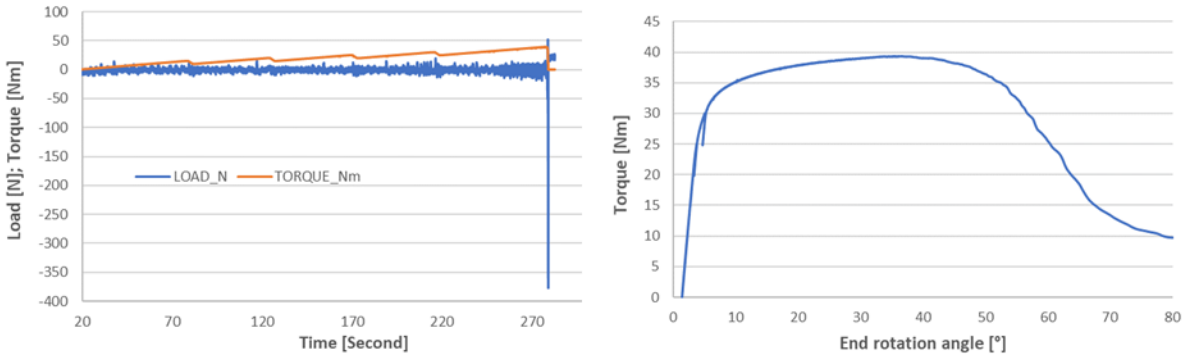

(b)

Fig. 9. (a) (left) Most SNTT weld 1-loop shallow-notch specimens' failures are initiated at HAZ regions, (right) All the weld 2-loop deep-notch specimens are failed at HAZ regions. (b) SNTT 2 loop Weld-8 specimen fracture test results, (left) Torque vs. angle data, sample failed at 39.5 N-m, and (right) Upon failure significant axial shock reaction load was observed, reaching magnitude of ~380 N.

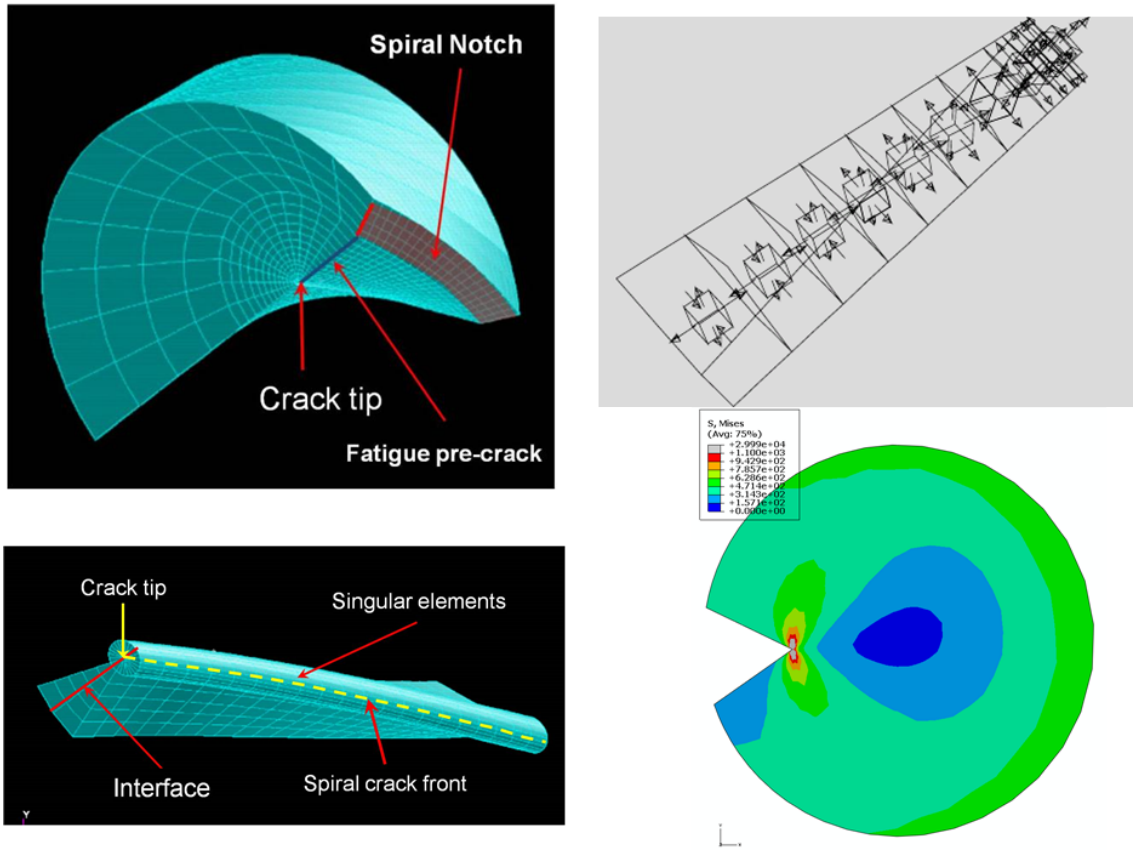

Fig. 10. (Left) Typical finite element models used for ductile material fracture toughness characterization, due to high ductility of the 304/308 weld material, the singular wedge element with quarter-node element around crack tip was relaxed back to normal wedge element with middle-node element; (Right) Typical FEM analyses results show tri-axial tensile stress profiles and butterfly plastic process zone near the crack front.

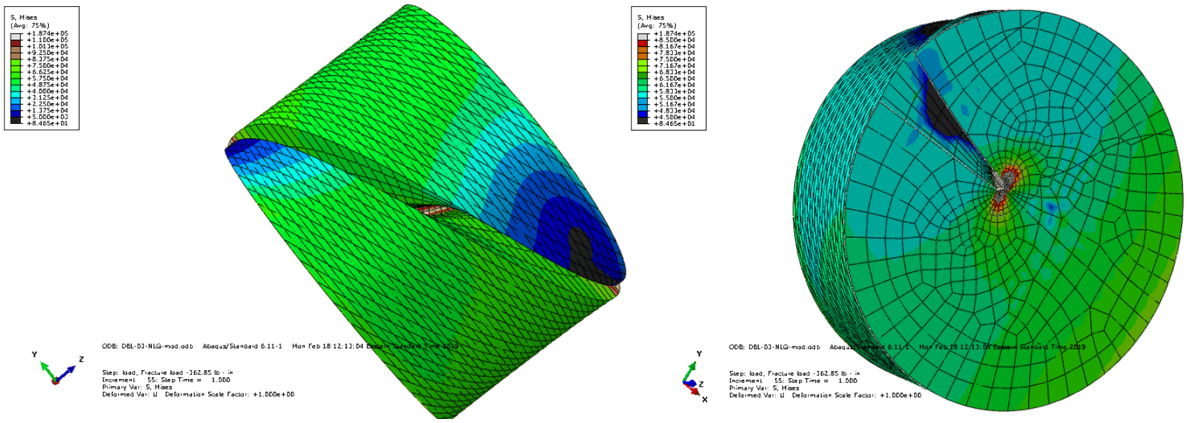

Fig. 11. SNTT Weld-10 specimen test FEA simulation (Left) Full model FEM deformation and von Mises stress profile, (Right) Deformation and von Mises stress profiles at near middle section of finite element model.

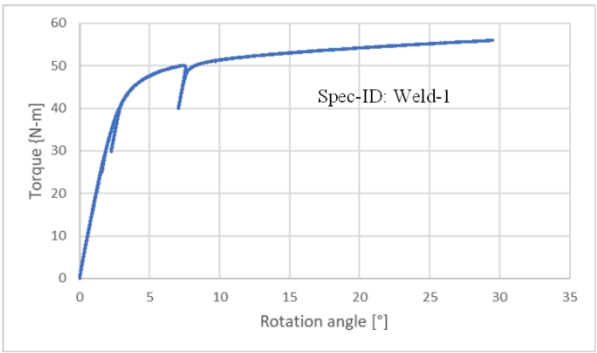

Maximum torque = 56.0 Nm

Area (N-m deg.°) = 1403.7 KJ-deg.°

Area (N-m rad.) = 24.5 KJ-radian

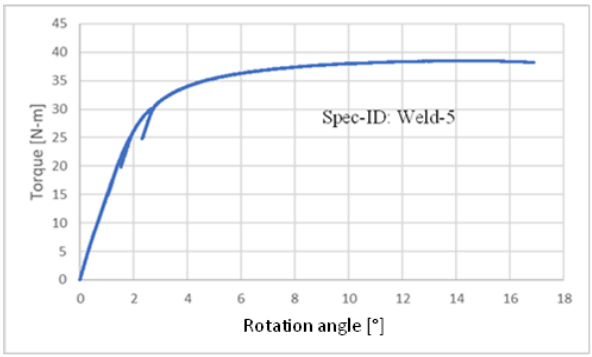

Maximum torque = 38.5 Nm

Area (N-m deg.°) = 547.7 KJ-deg.°

Area (N-m rad.) = 9.56 KJ-radian

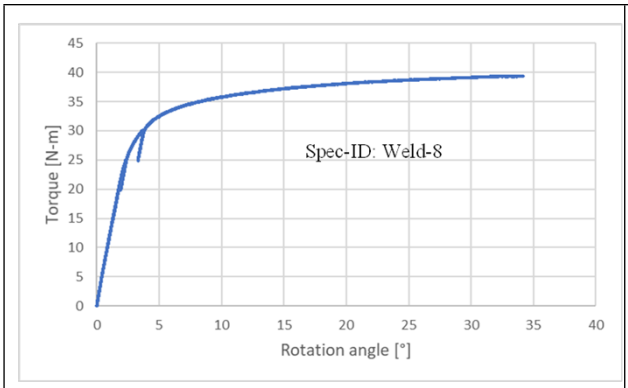

Maximum torque = 39.5 Nm

Area (N-m deg.°) = 1175.7 KJ-deg.°

Area (N-m rad) = 20.52 KJ-radian

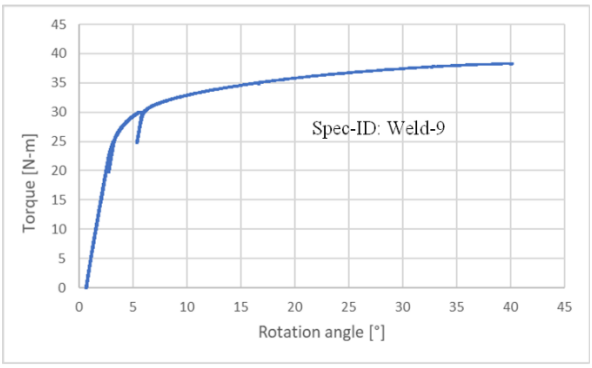

Maximum torque = 38.2 Nm

Area (N-m deg.°) = 1313.2 KJ-deg.°

Area (N-m rad) = 22.92 KJ-radian

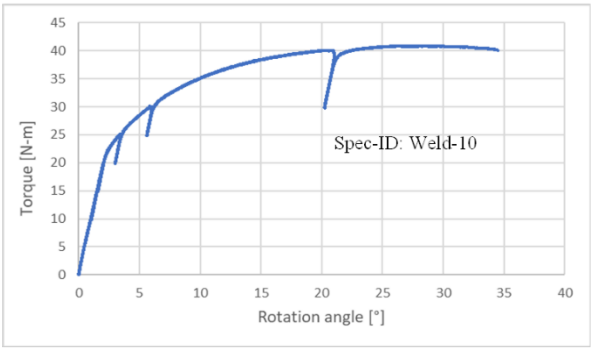

Maximum torque = 41.0 Nm

Area (N-m deg.°) = 1190 KJ-deg.°

Area (N-m rad) = 20.77 KJ-radian

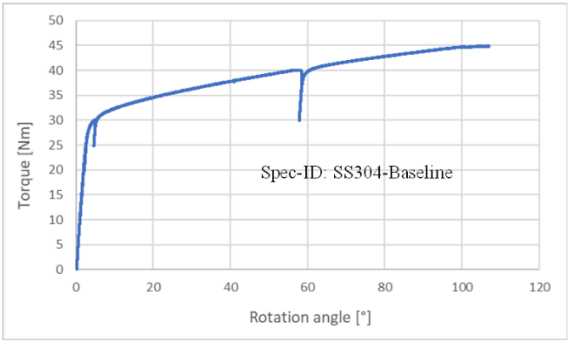

Maximum torque = 45.0 Nm

Area (N-m deg.°) = 4082 KJ-deg.°

Area (N-m rad) = 71.25 KJ-radian

Fig. 12 Plots of torque load versus rotation angle trend curve up to maximum fracture torque for the tested SNTT weld specimens.